Iraqi Journal for Applied Science (IJAS)
Vol. 3, No. 2, June, 2026, pp. 22-28
E-ISSN: 3006-5828 DOI: 10.69923/kezfk969

Research Article

Biosynthesis of $Fe_{1.83}Mn_{0.5}Zn_{0.41}O_4$ nanoparticles from milk thistle seed extract for use as anticancer agents

Zina.A.Al_Bader [1], Faten Zahran[2]

[1]Department of Biology, College of Education for Pure Sciences, University of Diyala, IRAQ.
[2]Faculty of Science, Department of Biochemistry. Zagazig University, Egypt.

Article Information

Article history:

Received: 26, 08, 2025
Revised: 22, 01, 2026
Accepted: 07, 05, 2026
Published: 30, 06, 2026

Keywords:

Fe1.83Mn0.5Zn0.41O4,
Nanoparticles,
Milk Thistle,
HL-60 cell line,
leukaemia cancer.

Abstract

This study employed a novel, simple, and cost-effective biosynthesis approach that combined co-precipitation, ultrasonic treatment, and green chemistry techniques to synthesize $Fe_{1.83}Mn_{0.5}Zn_{0.41}O_4$ nanoparticles using milk thistle (*Silybum marianum*) seed extract. The synthesized nanoparticles were characterized using Fourier Transform Infrared Spectroscopy (FT-IR), X-ray Diffraction (XRD), Energy-Dispersive X-ray Spectroscopy (EDX), Zeta Potential analysis, and Scanning Electron Microscopy (SEM). XRD analysis revealed an average crystallite size of 18.66 nm, whereas SEM analysis indicated an average particle size of 114.38 nm, suggesting particle aggregation. The anticancer activity of the synthesized $Fe_{1.83}Mn_{0.5}Zn_{0.41}O_4$ nanoparticles was evaluated against human leukemia HL-60 cell lines. The results demonstrated significant cytotoxic activity at higher nanoparticle concentrations, with a pronounced reduction in cell viability observed at concentrations of 500 and 1000 µg/mL. The percentages of viable cells at nanoparticle concentrations of 10, 25, 50, 100, 250, 500, and 1000 µg/mL were 85.98%, 83.56%, 84.54%, 98.41%, 97.87%, 29.04%, and 15.81%, respectively. The calculated IC_{50} value was 470.8 µg/mL. Statistical analysis using one-way ANOVA revealed highly significant differences among the treatment groups ($P < 0.0001$). The coefficient of determination ($R^2 = 0.9856$) indicated excellent model fitting and confirmed the strong relationship between nanoparticle concentration and biological response. The biocompatibility of the synthesized nanoparticles was further evaluated using a hemolysis assay with red blood cells at concentrations of 64, 128, and 256 µg/mL. The results showed no significant hemolytic activity or cytotoxic effects on erythrocytes, indicating that the synthesized nanoparticles were hemocompatible and safe within the tested concentration range.

Corresponding Author: Zina. A. AlBader, Department of Chemistry, College of Education for Pure Science, University of Diyala, Iraq, Baqubah City, Diyala Governorate, Iraq, ***Email***: pch.zina.alibader@uodiyala.edu.iq

1. INTRODUCTION

Nanomaterials have attracted considerable attention in recent years owing to their unique physicochemical properties and wide range of industrial, environmental, and biomedical applications [1]. The chemical and physical properties of nanoparticles are strongly influenced by their size, shape, morphology, and nanoscale composition. These distinctive characteristics have enabled their utilization in numerous fields, particularly in biomedical sciences [2]. Nanoparticles possess several advantageous features, including tunable structures, biocompatibility, ease of synthesis, and biomimetic behavior [3]. They have been extensively investigated for antimicrobial and antioxidant applications; however, their anticancer potential remains an active area of research. Cancer continues to be one of the leading causes of death worldwide, accounting for approximately 9.6 million deaths annually. Although surgery, chemotherapy, and radiotherapy remain the primary treatment modalities, each approach is associated with significant limitations and adverse effects [4].

The increasing use of nanomaterials in biomedicine and drug delivery systems has created a growing demand for safe, biocompatible, and environmentally sustainable synthesis methods. Several approaches have been developed for nanoparticle fabrication, including sol–gel synthesis [5], chemical vapor deposition, hydrothermal processing, and co-precipitation techniques [6]. Among these methods, green synthesis has attracted significant interest because it is simple, cost-effective, environmentally friendly, and minimizes the use of hazardous chemicals, solvents, and reducing agents [7]. Nanobiotechnology provides an alternative to conventional physical and chemical synthesis routes. Various biological resources, including bacteria, fungi, yeasts, viruses, and plant-derived materials such as leaves, roots, stems, and seeds, have been successfully utilized for the green synthesis of nanoparticles [8].

Among magnetic nanomaterials, nanoscale cubic spinel ferrites have attracted considerable scientific interest due to their superior magnetic and structural properties compared with their bulk counterparts. Depending on particle size and composition, spinel ferrites may exhibit single-domain structures and superparamagnetic behavior, making them highly attractive for technological and biomedical applications [9].

$ZnFe_2O_4$ is a typical spinel ferrite with the formula unit $(Zn^{2+})[Fe_2^{3+}]O_4$ [10]. In contrast, $MnFe_2O_4$ is a partially inverse spinel ferrite with the formula unit $(Mn_{0.8}^{2+}Fe_{0.2}^{3+})[Mn_{0.2}^{2+}Fe_{1.8}^{3+}]O_4$, indicating that approximately 80% of Mn^{2+} ions occupy tetrahedral sites, while the remaining ions are distributed within octahedral sites [11]. The magnetic and electrical properties of mixed $Mn_xZn_{1-x}Fe_2O_4$ spinel ferrites can be tailored by gradually substituting diamagnetic Zn^{2+} ions for magnetic Mn^{2+} ions. Owing to their high saturation magnetization, excellent permeability, and low core losses, Mn–Zn ferrites have found applications in transformer cores, magnetic amplifiers, recording heads, and other electronic devices [12,13]. Magnetic nanoparticles (MNPs) have been widely explored for biomedical applications, including targeted drug delivery, cellular labeling and tracking, gene therapy, magnetic hyperthermia, and magnetic resonance imaging (MRI) contrast enhancement [14]. For successful biomedical implementation, MNPs must exhibit low cytotoxicity, high colloidal stability under physiological conditions, and efficient loading and delivery capabilities for therapeutic agents or genetic materials [15]. Biological synthesis methods have gained increasing attention because they offer several advantages over conventional physical and chemical techniques, including environmental safety, reduced toxicity, mild reaction conditions, and the use of naturally occurring reducing and stabilizing agents. Nanoparticles synthesized through biological routes are generally more biocompatible, stable, and environmentally sustainable. Furthermore, plant-mediated synthesis allows the production of nanoparticles with controlled morphologies and sizes without the need for toxic chemical reagents [16,17].

Milk thistle (Silybum marianum) is one of the medicinal plants that has demonstrated promising pharmacological and anticancer activities. For centuries, milk thistle has been used in traditional medicine, particularly for the treatment of liver disorders, including toxin-induced liver damage, cirrhosis, hepatitis, and jaundice [18]. Although commonly referred to as seeds, the harvested structures are technically fruits; however, the term “seeds” is widely used in the literature and is therefore adopted in the present study [19]. Milk thistle, also known as Carduus marianus or wild artichoke, has gained considerable scientific interest over the last few decades [20]. One of the earliest reports suggesting its potential role in cancer prevention was presented by Mehta and Moon in 1991 [21], who demonstrated that silymarin acted as a chemopreventive agent against mammary carcinogenesis in mice exposed to dimethylbenz[a]anthracene (DMBA) and tetradecanoylphorbol acetate (TPA). Their findings indicated that silymarin exerted stronger chemopreventive effects during the tumor-promotion stage than during the initiation stage of carcinogenesis. In contrast, earlier pharmacological reviews primarily focused on the hepatoprotective properties of silymarin and did not extensively address its anticancer potential [22].

Therefore, the present study aimed to synthesize $Fe_{1.83}Mn_{0.5}Zn_{0.41}O_4$ nanoparticles through a novel, environmentally friendly green synthesis approach using milk thistle (Silybum marianum) seed extract and to evaluate their potential anticancer activity against selected cancer cell lines, including liver cancer and leukemia cells.

2. MATERIALS AND METHODS

2.1 Materials

The chemicals $Fe(NO_3)_3{\cdot}9H_2O$, $Zn(NO_3)_2{\cdot}6H_2O$, $Mn(NO_3)_2{\cdot}4H_2O$, Na_2CO_3, $NaBH_4$, ethanol (CH_3CH_2OH), castor oil, and deionized water were purchased from commercial suppliers and used without further purification. Milk thistle (*Silybum marianum*) seeds were obtained from a local market in Iraq. All chemicals used in this study were of analytical grade and high purity.

2.2 Preparation of Milk Thistle Seed Extract

Milk thistle seeds (50 g) were mixed with 500 mL of deionized water at a ratio of 1:10 (w/v). The mixture was heated and stirred continuously using a magnetic stirrer at 50°C for 1 h. The resulting extract was filtered using filter paper, and the filtrate was stored at 4°C until further use [23].

2.3 Biosynthesis of $Fe_{1.83}Mn_{0.5}Zn_{0.41}O_4$ Nanoparticles

To prepare the precursor solutions, 4.40 g of $Fe(NO_3)_3{\cdot}9H_2O$, 2.47 g of $Zn(NO_3)_2{\cdot}6H_2O$, and 2.10 g of $Mn(NO_3)_2{\cdot}4H_2O$ were each dissolved separately in 20 mL of milk thistle seed extract to obtain 0.5 M solutions. The three precursor solutions were then mixed and stirred magnetically at 50°C and 350 rpm for 30 min. Subsequently, 1 mL of castor oil was added to the mixture, followed by ultrasonic treatment for 15 min. After sonication, 6 mL of 1.5 M $NaBH_4$ solution was added dropwise under continuous stirring. The pH of the reaction mixture was adjusted to 7.5 using 3 M Na_2CO_3 solution. The resulting suspension was further stirred at 80°C and 350 rpm for 2 h. The precipitate formed was collected using a vacuum filtration system, washed three times with deionized water and twice with ethanol, and then dried at 180°C for 3 h. Finally, the dried product was calcined at 600°C for 4 h to obtain $Fe_{1.83}Mn_{0.5}Zn_{0.41}O_4$ nanoparticles.

2.4 MTT Cytotoxicity Assay

The cytotoxic activity of $Fe_{1.83}Mn_{0.5}Zn_{0.41}O_4$ nanoparticles was evaluated using the MTT assay. A stock solution of nanoparticles was prepared in 0.2% dimethyl sulfoxide (DMSO), and different concentrations were obtained through serial dilution. HL-60 leukemia cells were seeded in 96-well plates at a density of 1×10^4 cells per well in RPMI-1640 medium. The cells were incubated at 37°C in a humidified atmosphere containing 5% CO_2 for 24 h. After incubation, the cells were treated with different concentrations of $Fe_{1.83}Mn_{0.5}Zn_{0.41}O_4$ nanoparticles and incubated for an additional 24 h under the same conditions. Subsequently, 10 µL of MTT reagent (10 mg/mL) was added to each well and incubated for 5 h at 37°C. The absorbance was measured at 570 nm using a microplate reader, and cell viability percentages were calculated relative to untreated control cells [24].

2.5 Hemolysis Assay

The hemocompatibility of $Fe_{1.83}Mn_{0.5}Zn_{0.41}O_4$ nanoparticles was evaluated using a hemolysis assay. Fresh blood was collected from a healthy donor into an EDTA-containing tube under the supervision of qualified laboratory personnel. The blood sample was centrifuged at 1000 rpm for 10 min to separate plasma from blood cells. The plasma was discarded, and the red blood cells (RBCs) were washed three times with sterile phosphate-buffered saline (PBS). After washing, 1 mL of packed RBCs was diluted with 9 mL of PBS to obtain a homogeneous RBC suspension. Equal volumes of the RBC suspension and nanoparticle solutions at different concentrations were mixed and incubated for 2 h. PBS and distilled water were used as negative and positive controls, respectively. Following incubation, the samples were centrifuged at 1000 rpm for 5 min. Hemolysis was assessed by visual inspection of the supernatant. A red-colored supernatant indicated hemolysis and was considered a positive result, whereas a clear and colorless supernatant indicated the absence of hemolysis and was considered a negative result [25].

3. RESULTS AND DISCUSSION

3.1 FT-IR Characterization of $Fe_{1.83}Mn_{0.5}Zn_{0.41}O_4$ Nanoparticles

Fourier Transform Infrared Spectroscopy (FT-IR) is an effective technique for identifying the functional groups and vibrational characteristics of synthesized materials. Figure 1 presents the FT-IR spectrum of the biosynthesized $Fe_{1.83}Mn_{0.5}Zn_{0.41}O_4$ nanoparticles. Spinel ferrites typically exhibit four characteristic vibrational frequencies (ν_1, ν_2, ν_3, and ν_4), as reported by Waldron [26]. The ν_1 band, observed in the range of 500–600 cm^{-1}, corresponds to the stretching vibrations of Fe^{3+}–O^{2-} bonds at the tetrahedral sites. In the present study, a distinct absorption peak was observed at 550.88 cm^{-1}. The ν_2 band, which appears in the range of 350–450 cm^{-1}, is associated with the vibrations of metal–oxygen bonds (M^{2+}–O^{2-}), where M^{2+} may represent Zn^{2+}, Mn^{2+}, or Fe^{2+} ions occupying octahedral sites. A characteristic peak was observed at 470.94 cm^{-1} [26]. The higher vibrational frequency observed at tetrahedral sites compared with octahedral sites is attributed to the stronger Fe^{3+}–O^{2-} bond interactions and shorter bond lengths within the tetrahedral coordination environment [27]. Furthermore, the atomic mass and distribution of metal ions within the spinel lattice influence the observed vibrational frequencies [28].

3.2 XRD Characterization of $Fe_{1.83}Mn_{0.5}Zn_{0.41}O_4$ Nanoparticles

X-ray diffraction (XRD) analysis was employed to investigate the crystalline structure and phase purity of the biosynthesized $Fe_{1.83}Mn_{0.5}Zn_{0.41}O_4$ nanoparticles. As shown in Figure 2, the diffraction pattern closely matched the standard pattern reported in the International Centre for Diffraction Data (ICDD) card No. 96-152-8318 [29], confirming the successful formation of the $Fe_{1.83}Mn_{0.5}Zn_{0.41}O_4$ spinel ferrite phase. The diffraction peaks indicated a well-crystallized cubic spinel structure without detectable impurity phases. The average crystallite size calculated from the XRD data was 18.66 nm, confirming the nanocrystalline nature of the synthesized material.

3.3 EDX Characterization of $Fe_{1.83}Mn_{0.5}Zn_{0.41}O_4$ Nanoparticles

Energy-Dispersive X-ray Spectroscopy (EDX) was used to determine the elemental composition of the biosynthesized $Fe_{1.83}Mn_{0.5}Zn_{0.41}O_4$ nanoparticles. The EDX spectrum shown in Figure 3 confirmed the presence of the major constituent elements of the ferrite structure. The elemental analysis revealed the presence of Fe, Mn, and Zn with percentages of 51.79%, 13.00%, and 35.22%, respectively, indicating the successful incorporation of these elements into the synthesized ferrite nanoparticles. The absence of significant impurity peaks further suggests the high purity of the prepared material.

3.4 Zeta Potential Analysis of $Fe_{1.83}Mn_{0.5}Zn_{0.41}O_4$ Nanoparticles

The colloidal stability of $Fe_{1.83}Mn_{0.5}Zn_{0.41}O_4$ nanoparticles in aqueous media was evaluated using zeta potential measurements, as shown in Figure 4. Zeta potential is an important parameter that reflects the surface charge of nanoparticles and their tendency to remain dispersed in suspension. A higher absolute zeta potential value generally indicates stronger electrostatic repulsion between particles and improved colloidal stability. Nanoparticles with zeta potential values greater than approximately ±30 mV are typically considered stable in aqueous systems [30].

3.5 SEM Characterization of $Fe_{1.83}Mn_{0.5}Zn_{0.41}O_4$ Nanoparticles

The surface morphology and particle size distribution of $Fe_{1.83}Mn_{0.5}Zn_{0.41}O_4$ nanoparticles were investigated using Scanning Electron Microscopy (SEM). Representative SEM micrographs and particle size distribution histograms are presented in Figure 5. The SEM analysis revealed agglomerated particles with an average particle size of 114.38 nm, which is considerably larger than the average crystallite size of 18.66 nm obtained from XRD analysis. This difference can be attributed to the aggregation of multiple crystallites into larger particles due to their high surface energy and magnetic interactions. The observed agglomeration behavior is commonly reported in magnetic ferrite nanoparticles and results from strong interparticle magnetic attraction, leading to the formation of larger clusters. This phenomenon is clearly visible in the SEM micrographs.

3.6 Anticancer Activity of $Fe_{1.83}Mn_{0.5}Zn_{0.41}O_4$ Nanoparticles

The cytotoxic activity of biosynthesized $Fe_{1.83}Mn_{0.5}Zn_{0.41}O_4$ nanoparticles against HL-60 human leukemia cells was evaluated using the MTT assay. Cells were exposed to nanoparticle concentrations of 10, 25, 50, 100, 250, 500, and 1000 µg/mL for 48 h, and cell viability was assessed relative to untreated control cells. The percentages of viable cells were 85.98%, 83.56%, 84.54%, 98.41%, 97.87%, 29.04%, and 15.81% at concentrations of 10, 25, 50, 100, 250, 500, and 1000 µg/mL, respectively. A pronounced reduction in cell viability was observed at concentrations of 500 and 1000 µg/mL, indicating enhanced cytotoxic activity at higher nanoparticle concentrations. The calculated IC_{50} value was 470.8 µg/mL (Figure 7). Statistical analysis using one-way ANOVA revealed highly significant differences among treatment groups ($P < 0.0001$). Furthermore, the coefficient of determination ($R^2 = 0.9856$) demonstrated a strong concentration–response relationship. These findings indicate that $Fe_{1.83}Mn_{0.5}Zn_{0.41}O_4$ nanoparticles exhibit cytotoxic activity against HL-60 leukemia cells and may have potential applications in cancer-related biomedical research. Similar observations have been reported for magnetic nanoparticles used in drug delivery, diagnostic imaging, and anticancer applications [31–33].

3.7 Hemocompatibility Assessment of $Fe_{1.83}Mn_{0.5}Zn_{0.41}O_4$ Nanoparticles

The biocompatibility of $Fe_{1.83}Mn_{0.5}Zn_{0.41}O_4$ nanoparticles was evaluated through a hemolysis assay using red blood cells at concentrations of 64, 128, and 256 µg/mL. As shown in Figure 8, no evidence of hemolysis was observed at any of the tested concentrations, indicating that the synthesized nanoparticles exhibited good hemocompatibility and did not induce significant damage to red blood cells. According to the accepted classification of hemolytic activity, hemolysis rates ranging from 0–9% indicate non-toxic behavior, whereas values of 10–49%, 50–89%, and 90–100% correspond to slight, moderate, and severe toxicity, respectively [25]. The obtained results suggest that the synthesized $Fe_{1.83}Mn_{0.5}Zn_{0.41}O_4$ nanoparticles are biologically safe within the investigated concentration range and may be suitable for further biomedical applications.

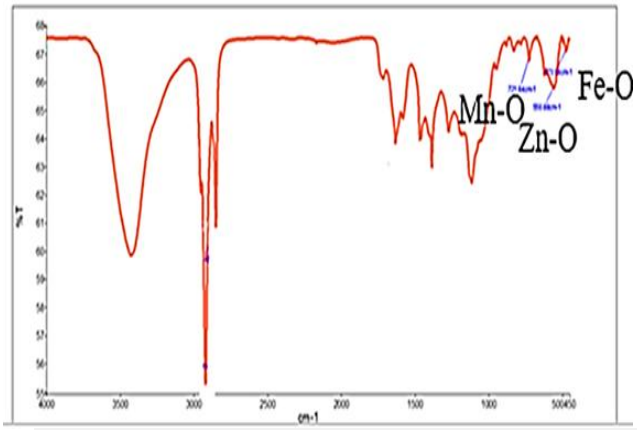

Figure 1. FT-IR Spectrum Fe1.83Mn0.5Zn0.41O4

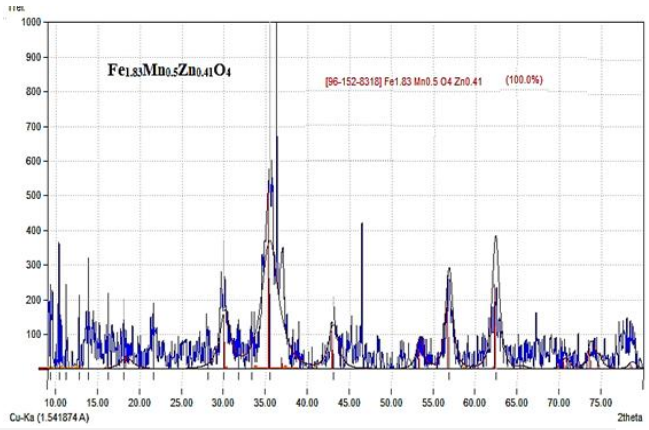

Figure2. XRD spectrum of Fe1.83Mn0.5Zn0.41O4

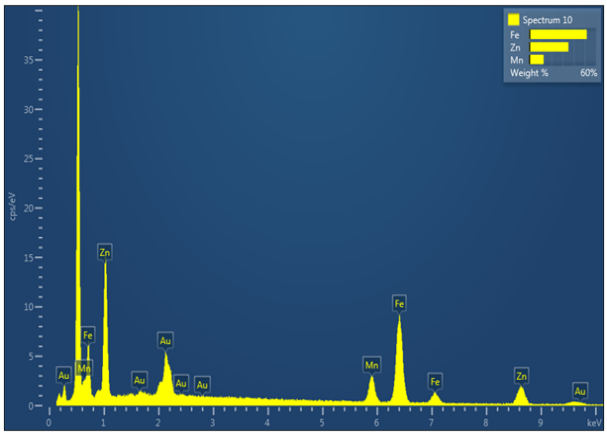

Figure 3. Diagnosis of Fe1.83Mn0.5Zn0.41O4by EDX

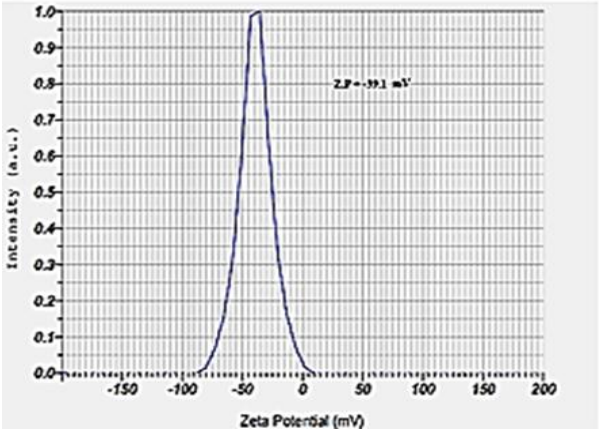

Figure 4. Zeta potential Fe1.83Mn0.5Zn0.41O4

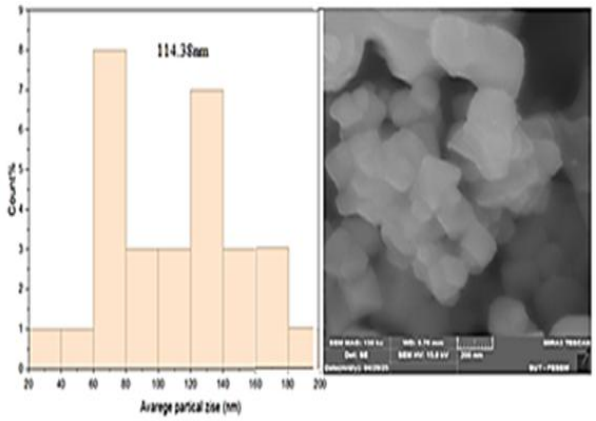

Figure 5. SEM of Fe1.83Mn0.5Zn0.41O4

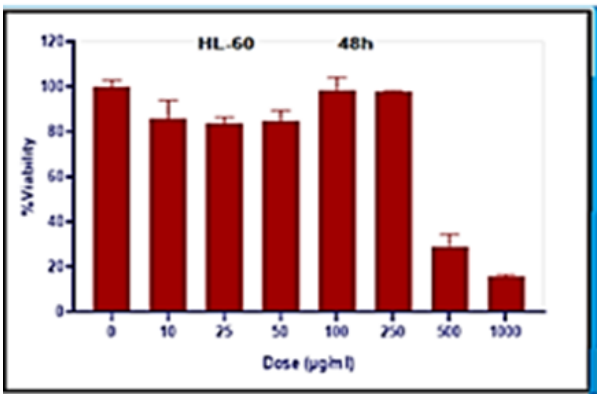

Figure 6. Viability of HL-60 cells treated with Fe1.83Mn0.5Zn0.41O4

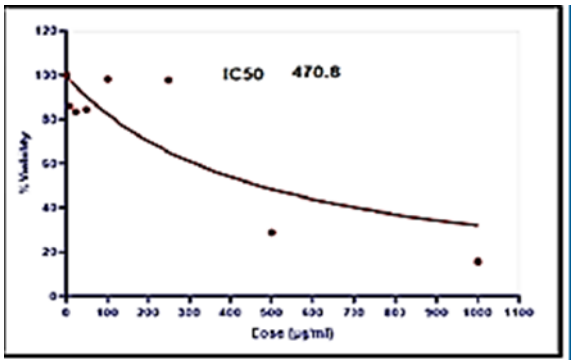

Figure 7. IC50 value calculation of Fe1.83Mn0.5Zn0.41O4

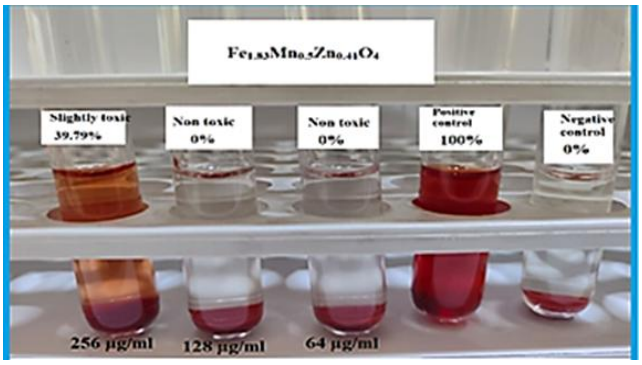

Figure 8. Toxicity Test of Fe1.83Mn0.5Zn0.41O4 NPs

3. CONCLUSION

In the present study, $Fe_{1.83}Mn_{0.5}Zn_{0.41}O_4$ nanoparticles were successfully synthesized using a novel, simple, cost-effective, and environmentally friendly biosynthesis approach that combined co-precipitation, ultrasonic treatment, and green chemistry techniques with milk thistle (Silybum marianum) seed extract. The synthesized nanoparticles were comprehensively characterized using FT-IR, XRD, EDX, zeta potential analysis, and SEM. XRD analysis confirmed the formation of a crystalline cubic spinel ferrite structure with an average crystallite size of 18.66 nm, whereas SEM analysis revealed an average particle size of 114.38 nm, indicating particle aggregation. The biological evaluation demonstrated that the synthesized nanoparticles exhibited cytotoxic activity against HL-60 human leukemia cells, particularly at higher concentrations. Cell viability decreased markedly at concentrations of 500 and 1000 µg/mL, and the calculated IC_{50} value was 470.8 µg/mL. Statistical analysis revealed highly significant differences among treatment groups ($P < 0.0001$), with a strong concentration–response relationship ($R^2 = 0.9856$). Furthermore, hemolysis studies performed at concentrations of 64, 128, and 256 µg/mL demonstrated no detectable toxic effects on red blood cells, indicating good hemocompatibility within the tested concentration range. Overall, the findings suggest that biosynthesized $Fe_{1.83}Mn_{0.5}Zn_{0.41}O_4$ nanoparticles possess promising physicochemical and biological properties that may support their future application in biomedical fields. Nevertheless, additional investigations involving apoptosis assays, molecular mechanism studies, and in vivo evaluations are required to further elucidate their therapeutic potential and biological safety.

REFERENCES

[1]. J. Jeevanandam, A. Barhoum, Y. S. Chan, A. Dufresne, and M. K. Danquah, "Review on Nanoparticles and Nanostructured materials: history, sources, Toxicity and Regulations," Beilstein Journal of Nanotechnology, vol. 9, no. 1, pp. 1050–1074, Apr. 2018, doi: https://doi.org/10.3762/bjnano.9.98.

[2]. H. R. Khan, Meena Kishore Sakharkar, A. Nayak, U. Kishore, and A. Khan, "Nanoparticles for biomedical applications: An overview," Elsevier eBooks, pp. 357–384, Jan. 2018, doi: https://doi.org/10.1016/b978-0-08-100716-7.00014-3.

[3]. M. Latha, M. Priyanka, P. Rajasekar, R. Manikandan, and N. M. Prabhu, "Biocompatibility and antibacterial activity of the Adathoda vasica Linn extract mediated silver nanoparticles," Microbial Pathogenesis, vol. 93, pp. 88–94, Apr. 2016, doi: https://doi.org/10.1016/j.micpath.2016.01.013.

[4]. H. Barabadi, M. Ovais, Z. K. Shinwari, and M. Saravanan, "Anti-cancer green bionanomaterials: present status and future prospects," Green Chemistry Letters and Reviews, vol. 10, no. 4, pp. 285–314, Oct. 2017, doi: https://doi.org/10.1080/17518253.2017.1385856.

[5]. R. Abbas et al., "Silver Nanoparticles: Synthesis, Structure, Properties and Applications," Nanomaterials, vol. 14, no. 17, p. 1425, 2024, doi: https://doi.org/10.3390/nano14171425.
[6]. A. F. Al-Alawy, E. E. Al-Abodi, and R. M. Kadhim, "Synthesis and Characterization of Magnetic Iron Oxide Nanoparticles by Co-Precipitation Method at Different Conditions," Journal of Engineering, vol. 24, no. 10, p. 60, Oct. 2018, doi: https://doi.org/10.31026/j.eng.2018.10.05.
[7]. M Haneefa, M Jayandran, and V. Balasubramanian, Asian Journal of Pharmaceutics, vol. 11, no. 1, Jan. 2017, doi: https://doi.org/10.22377/ajp.v11i01.1045.
[8]. N. E.-A. El-Naggar, M. H. Hussein, and A. A. El-Sawah, "Phycobiliprotein-mediated synthesis of biogenic silver nanoparticles, characterization, in vitro and in vivo assessment of anticancer activities," Scientific Reports, vol. 8, no. 1, Jun. 2018, doi: https://doi.org/10.1038/s41598-018-27276-6.
[9]. S. B. Singh et al., "Structural, thermal and magnetic studies of MgxZn1−xFe2O4 nanoferrites: Study of exchange interactions on magnetic anisotropy," Ceramics International, vol. 42, no. 16, pp. 19179–19186, Dec. 2016, doi: https://doi.org/10.1016/j.ceramint.2016.09.081.
[10]. "Smit, J. and Wijn, H.P.J. (1959) Ferrites. Philips Technical Library, Eindhoven, 150. - References - Scientific Research Publishing," www.scirp.org. https://www.scirp.org/reference/referencespapers?referenceid=1266992
[11]. M. M. Cruz et al., "Enhanced magnetic hyperthermia of CoFe2O4 and MnFe2O4 nanoparticles," Journal of Alloys and Compounds, vol. 703, pp. 370–380, May 2017, doi: https://doi.org/10.1016/j.jallcom.2017.01.297.
[12]. A. Amirabadizadeh, H. Farsi, M. Dehghani, and H. Arabi, "Effect of Substitutions of Zn for Mn on Size and Magnetic Properties of Mn–Zn Ferrite Nanoparticles," Journal of Superconductivity and Novel Magnetism, vol. 25, no. 8, pp. 2763–2765, Aug. 2011, doi: https://doi.org/10.1007/s10948-011-1259-5.
[13]. A. Angermann, J. Töpfer, K. L. da Silva, and K. D. Becker, "Nanocrystalline Mn–Zn ferrites from mixed oxalates: Synthesis, stability and magnetic properties," Journal of Alloys and Compounds, vol. 508, no. 2, pp. 433–439, Sep. 2010, doi: https://doi.org/10.1016/j.jallcom.2010.08.083.
[14]. N. T. K. Thanh and L. A. W. Green, "Functionalisation of nanoparticles for biomedical applications," Nano Today, vol. 5, no. 3, pp. 213–230, Jun. 2010, doi: https://doi.org/10.1016/j.nantod.2010.05.003.
[15]. K. E. Sapsford et al., "Functionalizing Nanoparticles with Biological Molecules: Developing Chemistries that Facilitate Nanotechnology," Chemical Reviews, vol. 113, no. 3, pp. 1904–2074, Feb. 2013, doi: https://doi.org/10.1021/cr300143v.
[16]. G. Nam, B. Purushothaman, S. Rangasamy, and J. M. Song, "Investigating the versatility of multifunctional silver nanoparticles: preparation and inspection of their potential as wound treatment agents," International Nano Letters, vol. 6, no. 1, pp. 51–63, Nov. 2015, doi: https://doi.org/10.1007/s40089-015-0168-1.
[17]. S. Ahmed, M. Ahmad, B. L. Swami, and S. Ikram, "A review on plants extract mediated synthesis of silver nanoparticles for antimicrobial applications: A green expertise," Journal of Advanced Research, vol. 7, no. 1, pp. 17–28, Jan. 2016, doi: https://doi.org/10.1016/j.jare.2015.02.007.
[18]. Philippe Lettéron et al., "Mechanism for the protective effects of silymarin against carbon tetrachloride-induced lipid peroxidation and hepatotoxicity in mice," vol. 39, no. 12, pp. 2027–2034, Jun. 1990, doi: https://doi.org/10.1016/0006-2952(90)90625-u.
[19]. R. Saller, R. Meier, and R. Brignoli, "The Use of Silymarin in the Treatment of Liver Diseases," Drugs, vol. 61, no. 14, pp. 2035–2063, 2001, doi: https://doi.org/10.2165/00003495-200161140-00003.
[20]. N. Vargas-Mendoza, "Hepatoprotective effect of silymarin," World Journal of Hepatology, vol. 6, no. 3, p. 144, 2014, doi: https://doi.org/10.4254/wjh.v6.i3.144.
[21]. R. G. Mehta and R. C. Moon, "Characterization of effective chemopreventive agents in mammary gland in vitro using an initiation-promotion protocol," Anticancer research, vol. 11, no. 2, pp. 593–6, 1991, Available: https://pubmed.ncbi.nlm.nih.gov/1905902/
[22]. Y. C. Rui, "Advances in pharmacological studies of silymarin," Memorias do Instituto Oswaldo Cruz, vol. 86 Suppl 2, pp. 79–85, 1991, doi: https://doi.org/10.1590/s0074-02761991000600020.
[23]. Areej Ali Jarullah, Mustafa Hammadi, and K. H. Hassan, "Green Synthesis of Nano Zn3(PO4)2 Using Curcuma Extract and Their Effect on SK-OV-3 Human Ovarian Cancer Cell Lines: Effects of Nano Zn3(PO4)2 at Human Ovarian Cancer Cell," Biological Sciences - PJSIR, vol. 68, no. 2, pp. 166–171, 2025, Accessed: Aug. 31, 2025. DOI: 10.52763/PJSIR.BIOL.SCI.68.2.2025.166.171.
[24]. H. S. Ahmed, M. Hammadi, and W. Majeed, "Green Synthesis of CuCr2O4Nano Composite from Rosemary Extract and Evaluation of its Anti-Breast Cancer Properties," Journal of Nanostructures, vol. 14, no. 4, pp. 1183–1190, Oct. 2024, doi: https://doi.org/10.22052/JNS.2024.04.018.
[25]. M. Pagano and C. Faggio, "The use of erythrocyte fragility to assess xenobiotic cytotoxicity," Cell biochemistry and function, vol. 33, no. 6, pp. 351–355, Aug. 2015, doi: https://doi.org/10.1002/cbf.3135.
[26]. R. D. Waldron, "Infrared Spectra of Ferrites," Physical Review, vol. 99, no. 6, pp. 1727–1735, Sep. 1955, doi: https://doi.org/10.1103/physrev.99.1727.
[27]. Ch. S. Lakshmi, Ch. S. L. N. Sridhar, G. Govindraj, S. Bangarraju, and D. M. Potukuchi, "Structural, magnetic and dielectric investigations in antimony doped nano-phased nickel-zinc ferrites," Physica B: Condensed Matter, vol. 459, pp. 97–104, Nov. 2014, doi: https://doi.org/10.1016/j.physb.2014.11.091.
[28]. M. Rahimi, P. Kameli, M. Ranjbar, H. Hajihashemi, and H. Salamati, "The effect of zinc doping on the structural and magnetic properties of Ni1−x Zn x Fe2O4," Journal of Materials Science, vol. 48, no. 7, pp. 2969–2976, Dec. 2012, doi: https://doi.org/10.1007/s10853-012-7074-y.

[29]. B. Antic, A. Kremenović, A. S. Nikolic, and M. Stoiljkovic, "Cation Distribution and Size-Strain Microstructure Analysis in Ultrafine Zn−Mn Ferrites Obtained from Acetylacetonato Complexes," The Journal of Physical Chemistry B, vol. 108, no. 34, pp. 12646–12651, Aug. 2004, doi: https://doi.org/10.1021/jp036214v.

[30]. M. Bloemen, W. Brullot, T. T. Luong, N. Geukens, A. Gils, and T. Verbiest, "Improved functionalization of oleic acid-coated iron oxide nanoparticles for biomedical applications," Journal of Nanoparticle Research, vol. 14, no. 9, p. 1100, Aug. 2012, doi: https://doi.org/10.1007/s11051-012-1100-5.

[31]. D. Chen et al., "Magnetic CuFe2O4 with intrinsic protease-like activity inhibited cancer cell proliferation and migration through mediating intracellular proteins," Biomaterials and Biosystems, vol. 5, pp. 100038–100038, Jan. 2022, doi: https://doi.org/10.1016/j.bbiosy.2021.100038.

[32]. H. Shagholani, S. M. Ghoreishi, and M. Mousazadeh, "Improvement of interaction between PVA and chitosan via magnetite nanoparticles for drug delivery application," International Journal of Biological Macromolecules, vol. 78, pp. 130–136, Jul. 2015, doi: https://doi.org/10.1016/j.ijbiomac.2015.02.042.

[33]. L.-W. Wang et al., "Quantum dots-based double imaging combined with organic dye imaging to establish an automatic computerized method for cancer Ki67 measurement," Scientific Reports, vol. 6, no. 1, Feb. 2016, doi: https://doi.org/10.1038/srep20564.

[34]. S. N. Kang, M. H. Lee, K.-M. Kim, D. Cho, and T. S. Kim, "Induction of human promyelocytic leukemia HL-60 cell differentiation into monocytes by silibinin: involvement of protein kinase C," Biochemical Pharmacology, vol. 61, no. 12, pp. 1487–1495, May 2001, doi: https://doi.org/10.1016/S0006-2952(01)00626-8.

BIOGRAPHIES OF AUTHORS

	**Dr. Faten Zahran** is a Professor at the Faculty of Science, Department of Biochemistry. Zagazig University, Egypt. Her holds a PhD degree in Chemistry Science with a specialization in Biochemistry and Biolog. Her has published several scientific papers in national and international conferences and journals. Her can be contacted by email: fzahran@science.zu.edu.eg
	Scopus
	**Zina A. Al-Bader** is a Master's student at the Department of Chemistry, College of Education for Pure Science, University of Diyala, Iraq. He received a B.Sc. in Chemistry from the College of Education for Pure Sciences, Ibn Al-Haytham University of Baghdad. His research areas are nanoscale inorganic materials, their characterization, and biological effectiveness studies. He can be contacted by email. pch.zina.alibader@uodiyala.edu.iq
	Scopus